Molecular Crystals and Liquid Crystals Science and Technology. Section A. Molecular Crystals and Liquid Crystals

Publication details, including instructions for authors and subscription information:
http://www.tandfonline.com/loi/gmcl19

Optical Probes of C_{60} Thin Films

R. E. Benner [a], D. Dick [a], X. Wei [a], S. Jeglinski [a], Z. V. Vardeny [a], D. Moses [b], V. I. Srdanov [b] & F. Wudl [b]

[a] Departments of Electrical Engineering and Physics, University of Utah, Salt Lake City, Utah, 84112, U.S.A.

[b] Institute of Polymers and Organics Solids University of California, Santa Barbara, California, 93106, U.S.A.

Version of record first published: 04 Oct 2006.

To cite this article: R. E. Benner , D. Dick , X. Wei , S. Jeglinski , Z. V. Vardeny , D. Moses , V. I. Srdanov & F. Wudl (1994): Optical Probes of C_{60} Thin Films, Molecular Crystals and Liquid Crystals Science and Technology. Section A. Molecular Crystals and Liquid Crystals, 256:1, 241-250

To link to this article: http://dx.doi.org/10.1080/10587259408039253

Mol. Cryst. Liq. Cryst. 1994, Vol. 256, pp. 241–250
Reprints available directly from the publisher
Photocopying permitted by license only

OPTICAL PROBES OF C_{60} THIN FILMS

R.E. BENNER, D. DICK, X. WEI, S. JEGLINSKI, AND Z.V. VARDENY
Departments of Electrical Engineering and Physics
University of Utah, Salt Lake City, Utah 84112 U.S.A.

and

D. MOSES, V.I. SRDANOV, AND F. WUDL
Institute of Polymers and Organics Solids
University of California, Santa Barbara, California 93106 U.S.A.

Abstract Data obtained from thin films of C_{60} using the techniques of absorption, photoluminescence, resonance Raman scattering, electroabsorption, and transient photomodulation are presented to develop an understanding of the energy levels and their dynamics in this fullerene solid.

INTRODUCTION

Since the fullerenes, in particular C_{60}, became available in quantity,[1] they have stimulated a large amount of experimental and theoretical work. The C_{60} molecules, with icosahedral symmetry, condense at room temperature into a FCC Bravais lattice held together by rather weak intermolecular van der Waals forces, with a high degree of rotational disorder[2]. Band-structure calculations show that C_{60} solid is a molecular semiconductor with a direct band-gap (E_g) of 1.5 eV between narrow (~0.5 eV) continuum bands[3]. The optical transitions between the analogous states in C_{60} molecules are dipole forbidden, but they are weakly allowed in the solid form[4]. However, recent photoemission and inverse-photoemission[5], and ellipsometric[6] spectra of C_{60} films indicate that $E_g = 2.3$ eV. The weak optical absorption in the range of 1.6 to 2.2 eV[7] (Fig. 1) must therefore correspond to intramolecular Frenkel-type excitons[5]. The character of the primary photoexcitations and their decay channels, and the properties of long-lived charged and neutral photoexcitations in C_{60} solids are therefore of interest. Similar results for thin films of C_{70} and their comparison with those of C_{60} can provide further insight on the underlying mechanisms for these properties.

EXPERIMENTAL TECHNIQUES

Thin films of purified C_{60} and C_{70} were evaporated (at 450° C and 5×10^{-6} Torr[8]) onto sapphire or glass substrates to a thickness of approximately 1000 angstroms. Unpolarized Raman spectra were collected in a backscattering geometry using a Spex 0.85 meter double monochromator equipped with a GaAs photomultiplier and photon counting electronics. The instrumental resolution was 4 cm^{-1}. A Spex triple spectrograph equipped with a Photometrics CCD array was also used. Various Ar^+ laser lines and an Ar^+-pumped dye laser were used to provide excitation in the range from 2.0 to 2.7 eV. Approximately 30 mW of laser light was focused with a cylindrical lens to a 100 μm by 4 mm spot on the sample. All of the Raman spectra were collected at room temperature with the sample constantly exposed to air. This approach was used because the photoinduced changes in the Raman spectrum have been shown to saturate after a few minutes under these conditions[9]. In addition, Raman spectra from a sample kept in vacuum gave similar results. The Raman spectra were all collected from a single spot on the sample which had been irradiated to reach a steady state. A small industrial diamond was mounted adjacent to the sample on a translation stage, and the scattering efficiencies were measured relative to the diamond 1332 cm^{-1} line.

For the EA measurements aluminum electrodes were first deposited on a sapphire substrate in an "interlocking finger" geometry. A gap of 20 μm between adjacent electrodes allowed the use of voltages less than 200 V_{rms} to achieve the required field strengths of 10^4 - 10^5 Vcm^{-1}. A small sine-wave voltage was connected to a custom-built step-up transformer, the output of which was connected to the electrode. The electrode was housed inside a cryostat for experiments between 80K and 300 K. The electric-field modulation frequencies ranged from 250 Hz to 1 kHz A light source (100W tungsten lamp for the visible, 450W Xe lamp for the ultraviolet) was focused on a computer-controlled .25 meter f/4 monochromator, whose output was directed through a mechanical chopper, focused on the sample, and detected by a UV-enhanced silicon photodiode. This configuration was used to minimize any photodegradation of the C_{60} sample[10]. The photodiode electrical output was directed to a computer-controlled lock-in amplifier. For each spectrum, the transmission (T) was measured with the mechanical chopper in place and the electric field off. The differential transmission (ΔT) was subsequently measured without the chopper and with the electric field on, with the lock-in set to detect signals at twice the electric-field modulation frequency. The data were divided to yield the $-\Delta T/T$ information, which is free of the spectral response function.

The spectral evolution of the excited states in the picosecond time domain was studied by the pump-and-probe correlation technique using two dye lasers

synchronously pumped by a frequency-doubled modelocked Nd:YAG laser at a repetition rate of 76 MHz, and by a streak camera with 10 ps resolution for the PL transient. The dye laser system had a pump-probe cross correlation of about 5 ps. Transient spectra of photoinduced changes ΔT in transmission T were obtained by fixing the pump wavelength at 570 nm (2.17 eV) and varying the probe wavelength between 1.2 and 2.2 eV with a sensitivity in $\Delta T/T$ of 3×10^{-6} [11]. For transient photomodulation (PM) measurements in the femtosecond time domain we used a colliding pulse modelocked (CPM) dye laser with 60 fs pulse duration at 620 nm (2 eV).

The time interval between 1 μs to 50 ms was studied using a cw PM apparatus[12]. The excitation was an Ar^+ laser beam modulated at frequency f between 20 Hz and 1 MHz by an acousto-optic modulator, and the probe beam source was a premonochromatized incandescent lamp in the spectral range of 0.25 to 2.6 eV. $\Delta T(f)$ was measured by a set of fast detectors with matched preamplifiers and a lock-in amplifier. For excitation spectra of various PA bands in the PM spectra, ΔT at a single probe energy was measured as the film was photoexcited with photon energies from 1.5 to 4.5 eV. The quantum efficiency (QE) spectrum was calculated by normalizing the excitation spectrum by the number of absorbed phonons.

RESULTS

A. Absorption and Raman Spectra

Figure 1 compares the optical density of a solution of C_{60} molecules to that of a thin film of C_{60}. Peaks in the film tend to be broadened and red-shifted compared to the solution

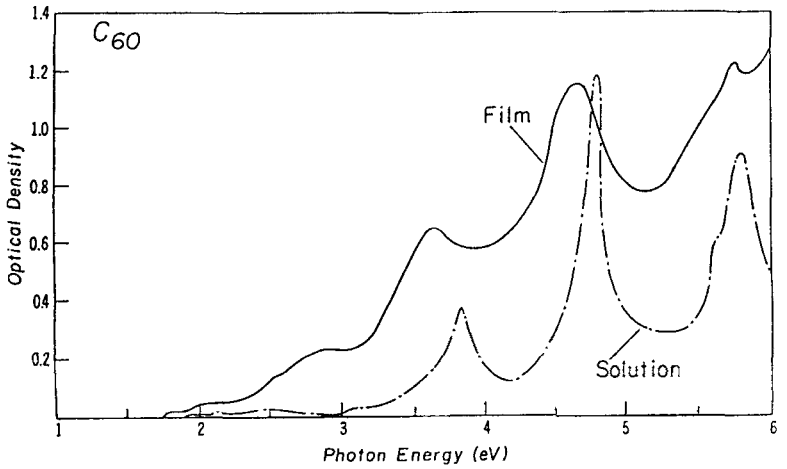

Fig. 1. The absorption spectrum of C_{60} solution compared to that of a C_{60} film.

data. In addition, the film data exhibit a small, but significantly increased absorption in the bandgap region near 2.3 eV where solid-state effects are observed. Absorption data for C_{70} films show similar behavior with somewhat greater absorption in the bandgap region near 2.1 - 2.2 eV.

As shown in the inset of Fig. 2, the Raman spectrum of C_{60} includes two major A_g peaks near 496 and 1469 cm^{-1}. The Raman intensity of the C_{60} 1469 cm^{-1} line (Fig. 2) shows a moderate resonant enhancement at 2.4 eV. The 496 cm^{-1} line shows a similar but smaller enhancement at this energy. In addition, a shoulder in the C_{60} enhancement spectrum extends toward lower energy to approximately 1.8 eV and then rapidly decreases. The Raman excitation profile of C_{70} shows a peak at 2.2 eV for the 1231 cm^{-1} and 1568 cm^{-1} lines. The group of lines between 1445 cm^{-1} and 145 cm^{-1}, which were not completely resolved, remained constant in intensity over our range of excitation energies.

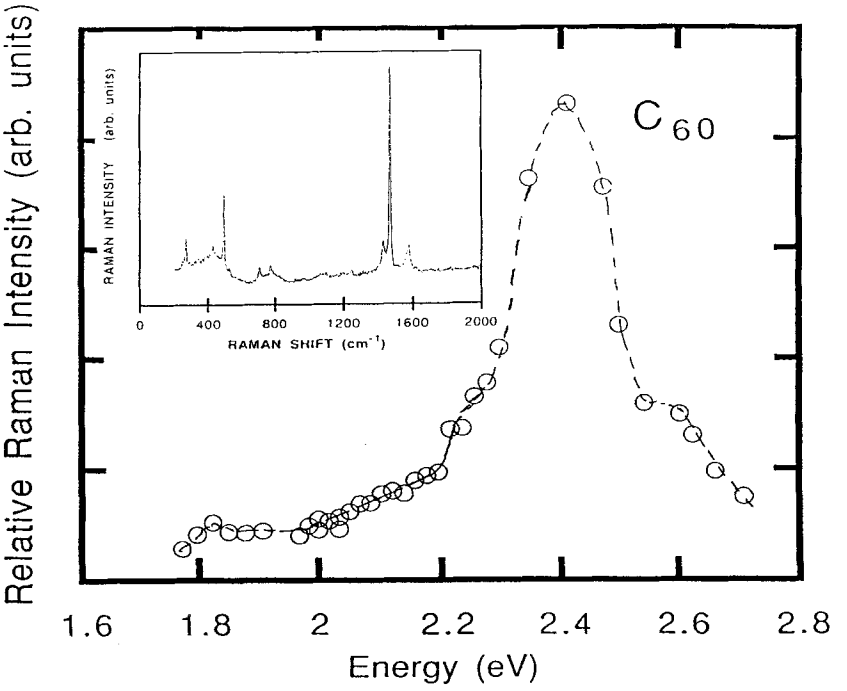

Fig. 2. Resonant Raman scattering profile of a C_{60} film. Inset shows a typical Raman spectrum.

B. PL and EA Spectra

As shown in Fig. 3, the photoluminescence (PL) excitation profile for the C_{60} film was qualitatively similar to the Raman excitation profile. The onset of PL emission for C_{60} occurs near 1.9 eV, peaks near 1.8 eV, and extends to near 1.2 eV. Similar to the Raman excitation profile, the PL excitation spectrum peaks near 2.3 eV. The PL excitation spectrum for a C_{70} film peaks near 3.2 eV, but extends with high quantum efficiency to below 2 eV.

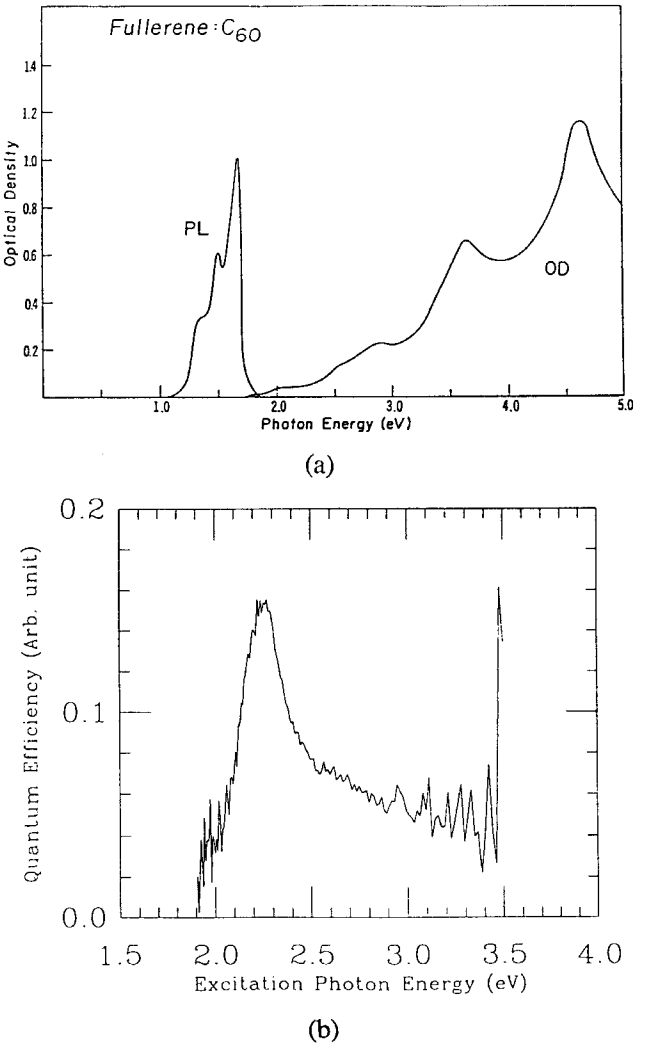

Fig. 3. Photoluminence of C_{60} film (a) photoluminescence emission compared to absorption (b) photoluminescence excitation measured at emission peak.

Electroabsorption (EA) data for a thin film of C_{60} are shown in Fig. 4. For C_{60}, in contrast to the featureless optical density, a large derivative-like feature is observed centered about the bandgap energy at 2.3 eV indicating a high polarizability. When integrated over the energy range from 1.8 to 2.6 eV the EA results qualitatively match the Raman and PL excitation profiles in this range. The EA of a C_{70} film also has a strong derivative-like feature near the bandgap at 2.2 eV, but exhibits strong exciton peaks toward lower energies, which are more pronounced than in C_{60}.

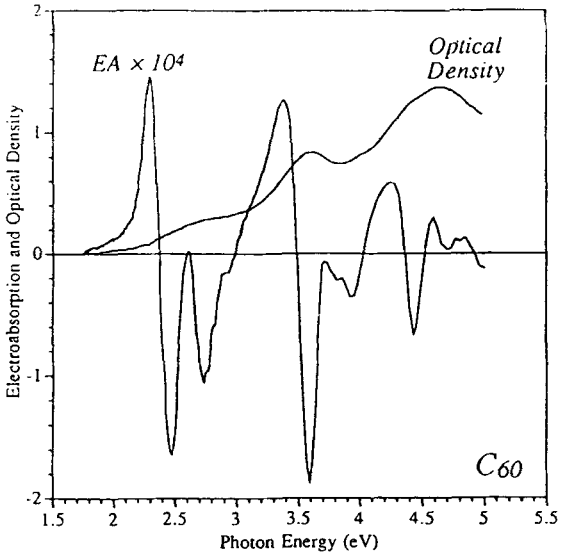

Fig. 4. Electroabsorption spectrum of C_{60} film compared to its optical density.

C. Picosecond PM Spectra

The transient PM spectrum of a C_{60} film obtained with the synchronously pumped system at 300 K, with initial photoexcitation density of ~10^{17} cm^{-3}, is shown in Fig. 5 for time delay t = 0. We observe a PA band with a broad maximum at about 1.8 eV and a width of 0.4 eV. Using the CPM laser, we found that the PA band is formed instantaneously; no initial photobleaching is observed [13,14]. This shows that the PA response is dominated by the excited state absorption, consistent with the weak absorption at the excitation photon-energy (Fig. 1). The PA spectrum of the photoexcitations remains essentially unchanged up to 3ns. For example, the spectrum at 2 ns is compared to that at t = 0 in Fig. 5. We infer from the similarity of the two spectra that the dominant photoexcitations at 3 ns are the same as those generated at 100 fs.

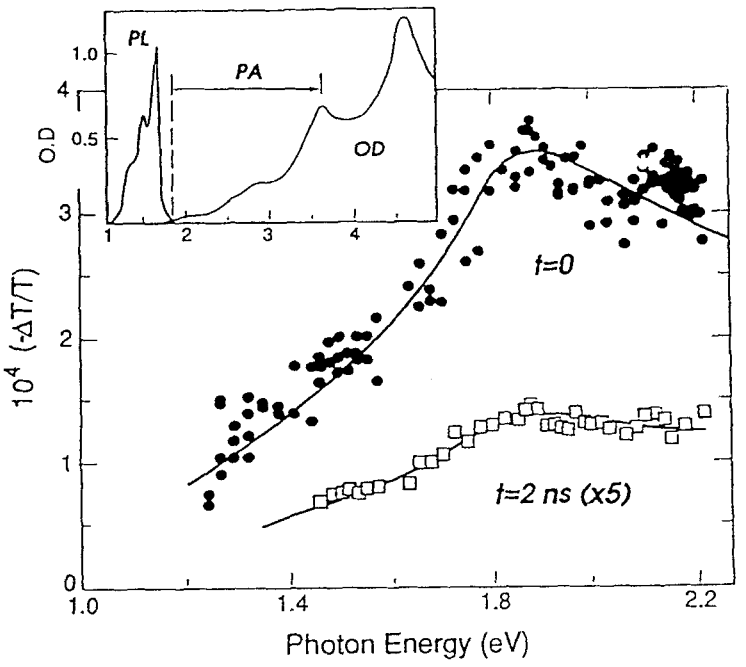

Fig. 5. Picosecond PA spectra of C_{60} film at t=0 (5 ps resolution) and t=2 ns; the lines through the data points are to guide the eye. The inset shows the film's optical absorption spectrum and the PL band.

D. CW PM Spectra

Fig. 6 shows the transient PA spectra from 0.25 to 2.6 eV at different modulation frequencies (f) and temperatures (θ). We see that within the spectral range of the ps measurements (1.2 to 2.2 eV) there are now at least five PA features as shown in Fig. 6(b). These are PA bands C_1 and C_2 at 0.8 and 2 eV respectively, T_1 and T_2 at 1.2 and 1.8 eV, respectively, and a derivative-like feature (E) with zero crossing at 2.4 eV. We find that all PA bands increase as $I_L^{1/2}$, indicating a bimolecular recombination kinetics. However, the various PA bands do not share a common origin because of their distinctly different dependencies on f and θ. C_1, C_2 and E vary more strongly with f than T_1 and T_2 (Figs. 5(a) and 5(b)). Also T_1 and T_2 have a stronger θ dependence than C_1, C_2, and E, demonstrated by the complete disappearance of T_1 and T_2 from the PM spectrum at θ = 300 K (Fig.6(a)).

The inset of Fig. 6(c) shows our electro-absorption (EA) spectrum [15] measured at 300 K on the same C_{60} film. As mentioned above the EA spectrum shows strong derivative-like features [15,16] caused by excitonic stark shifts. We note that the lowest

energy feature is identical with band E in the PM spectrum, leading us to identify this feature as due to EA. The source of the electric field is photoinduced charge separation in the film. Since the band E is more correlated with C_1 and C_2, we tentatively identify the C_1 and C_2 PA bands as being due to photogenerated charge carriers. The T_1 and T_2 PA bands, on the other hand, are due to neutral photoexcitations, probably long-lived triplet excitons.

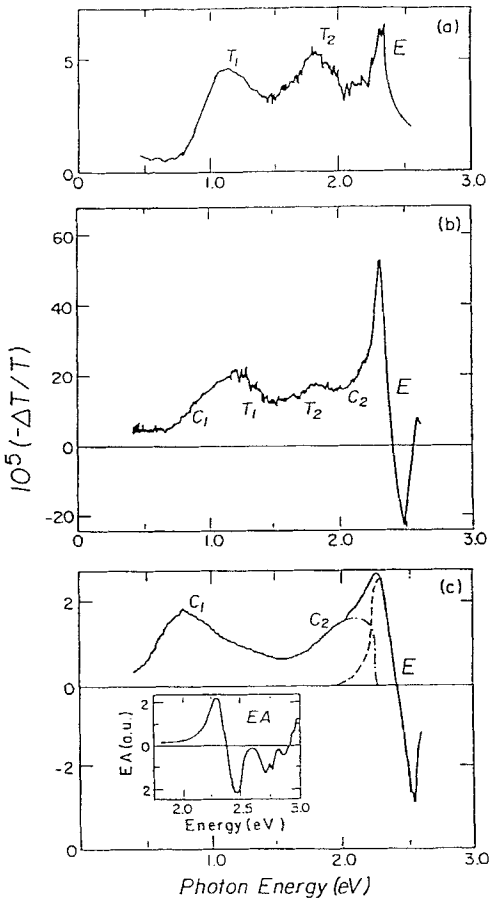

Fig. 6. PM spectra of C_{60} film at different modulation frequency f and sample temperature θ. (a) f = 20 kHz, θ = 80 K; (b) f = 20 Hz, θ = 80 K; (c) f = 500 Hz, θ = 300 K. The PA bands C_1, C_2, T_1, T_2, and E are assigned. The inset in Fig. 6 (c) shows the electroabsorption spectrum measured on the same C_{60} films.

DISCUSSION

Like another well known and extensively studied semiconductor, Cu_2O, the optical properties of C_{60} solid are not easily understood. This stems from the fact that the HOMO-LUMO transition in C_{60} molecules is dipole forbidden based on symmetry (A_g to T_{2g} transition). The question of how this strictly forbidden selection rule relaxes in the solid state is very intriguing. Another important question involves the rates of other, weaker transitions in determining the characteristic optical properties of C_{60} solid. In our laboratory we have used a variety of optical probes to answer these questions.

C_{60} solid forms electronic bands rather than electronic levels as in C_{60} molecules. This can be easily observed when comparing their respective $\alpha(\omega)$ spectra. Next the location of the interband transition becomes a question. Based on the excitation spectra of photoconductivity, charge excitations in the PM spectrum, and resonance Raman scattering (RRS), we speculate that the band gap E_g = 2.3 eV. The latter spectrum (RRS) is very revealing since it places the first really allowed transition caused by solid state effects at about 2.4 eV. This is above E_g = 2.3 eV, probably because of the progressively relaxed dipole moment transition inside the continuum band. Below E_g we expect a series of "dark" excitons; i.e., with forbidden transitions to the ground state (GS).

The lowest lying such exciton is probably at 1.8 eV. This can be inferred from the RRS excitation spectrum (Fig. 2) with an onset at 1.8 eV, the onset of the PL emission band, and the onset of $\Delta\alpha > 0$ in the EA spectrum (Fig. 4). Since the binding energy E_b of this lowest exciton is of order 0.5 eV, this puts enough constraints on its wavefunction to be intramolecular Frenkel-type exciton. But the exciton character may change for excitons with higher energies in the below-gap exciton series. Probably the highest exciton in this series is at 2.25 eV. This can be inferred from the pronounced band at 2.25 eV in the PL excitation spectrum, and the derivative like spectral feature in EA at this energy. Since the E_b of this exciton is less than 100 meV, we expect it to have a more intermolecular character.

Our results for excited states in C_{60} films can be explained by the following scenario. Upon excitation below the gap, singlet excitons are formed. Since they are of T_{2g} character, transitions into the various excited states with T_{2u} character are allowed. One of them should occur between the lowest Frenkel exciton at 1.8 eV and the 3.6 eV peak in the $\alpha(\omega)$ spectrum. This explains the picosecond PA spectrum (Fig. 5) with a PA band at 1.8 eV as caused by excitons. At low densities these excitons recombine geminately; some of them decay radiatively giving rise to the fast PL component. A small fraction of the singlet excitons decay into the triplet manifold at $t >> 3$ ns.

Although fast triplet recombination occurs via bimolecular kinetics, some $C_{60}^{\pm}$ maybe also produced by charge separation, which probably contributes to the slow PC component[17].

ACKNOWLEDGMENTS

The work at the University of Utah was supported in part by the DOE grant no. DE-FG 03-93 ER 45490 and by ONR grant no. N00014-91-C-0104. The work at UCSB was supported by NSF-DMR 90-12808. V.I.S. acknowledges support by the NSF QUEST program at UCSB. We also acknowledge fruitful discussions with E. Rashha and J. Worlock.

REFERENCES

1. W. Krätschmer, L. D. Lamb, K. Fostiropoulos and D. R. Huffman, Nature 397, 354 (1990).
2. P. Heiney, et al., Phys. Rev. Lett. 66, 2911 (1991).
3. S. Saito and A. Oshiyama, Phys. Rev. Lett. 66, 2637 (1991).
4. W. Y. Ching, et al., Phys. Rev. Lett. 67, 2045 (1991).
5. R. W. Lof, et al., Phys. Rev. Lett. 68, 3924 (1992).
6. S. L. Ren, et al., Appl. Phys. Lett. 59, 2678(1991).
7. A. Skumanich, Chem. Phys. Lett. 182, 486 (1991).
8. R. E. Haufter, et al., J. Phys. Chem., 94, 8634 (1990).
9. S. J. Duclos, et al., Solid State Comm., 80, 481 (1991).
10. R. Taylor, et al., Nature, 351, 277 (1991).
11. G. S. Kanner, Ph.D. thesis, University of Utah, 1991 (unpublished).
12. X. Wei, B. C. Hess, Z. Vardeny, and F. Wudl, Phys. Rev. Lett., 68, 666 (1992).
13. R. A. Cheville and N. J. Halas, Phys. Rev. B., 45, 4548 (1992).
14. S. D. Brorson, et al., Phys. Rev. B., 46, 7329 (1992).
15. S. Jeglinski, et al., J. Synth. Metals, 50, 557 (1992).
16. K. Pichler, et al., J. Phys. C; Condens. Matter, 3, 9259 (1991).
17. C. H. Lee, D. Moses, V. I. Srdanov and F. Wudl, Phys. Rev. B., (in press).